*Acta Cryst.* (1948). 1, 238

# Analyses and Interpretations of X-ray Diffraction Effects in Patterns of Aged Alloys

By A. H. Geisler and Miss J. K. Hill

*General Electric Research Laboratory, Schenectady, New York, U.S.A.*

(*Received* 27 *February* 1948)

The limitations of the various X-ray diffraction methods which have been used to study the structure of aged alloys are discussed. A method which employs a stationary single crystal and characteristic radiation is described. The method is applied to the structures in aged Al–Ag and Al–Mg–Si alloys. Evidence for one- and two-dimensional diffraction is reported for both alloys. Limitation of particle dimensions is proposed as a general explanation of the diffraction effects; this is the most suitable explanation for patterns of Al–Mg–Si alloys. Reciprocal-lattice points for thick particles of the precipitate structure evolve from rods for thin platelets, and evolve earlier from planar areas in the reciprocal lattice corresponding to particles that have only one resolvable dimension. A change in structure to that of the precipitate has occurred at the earliest detectable stage. Indefinite periodicities in the matrix structure cannot account for the data for either this alloy or for a previously studied Al–Mg alloy. The interpretation based on particle size is also adequate for other alloy systems, such as Al–Cu and Al–Ag, in which the diffraction effects of the precipitate are more intimately related to those of the matrix. The existence of predominantly one-dimensional particles prior to the platelike particles in the sequence of growth is identified. This is a new concept in the theory of the precipitation process.

## 1. Introduction

The detection of precipitation in aged alloys has been constantly subjected to the limitations of the various methods of examination. These have at times imposed interpretations that confused the basic understanding of precipitation mechanism and age-hardening. The limitations of the light microscope were recognized early, since the failure to detect precipitate in age-hardened alloys was attributed to the submicroscopic size of the particles. Limitations of X-ray methods, however, were not so quickly recognized. When back-reflection methods failed to reveal changes in the lattice parameter of the matrix solid solution during age-hardening, theories based on the agglomeration of solute atoms into clusters or 'knots' in the matrix structure were advanced. Distinctions were made between 'cold aging' and 'hot aging', for at low aging temperatures the hardness increased without detectable evidence of precipitation, whereas only aging at elevated temperatures provided the expected change in the lattice parameter. In the meantime polishing and etching methods improved to the point that definite evidence of precipitation could be detected microscopically at shorter aging intervals than those at which the lattice parameter change became apparent. The low sensitivity of the powder method was thus proven. The detection has been considerably extended by the electron microscope, but even this tool has its limitations.

At present the most powerful method for studying the precipitate particles when they are still very small appears to be the X-ray diffraction techniques that employ single, matrix crystals. When the limitations are recognized, the diffraction effects at the very earliest stages of precipitation can be interpreted as evidence for precipitate particles which are only a few unit cells in size. Anisotropic growth can be followed until the particles exceed the size in all dimensions necessary for sharp diffraction effects. Interpretations involving pre-precipitation phenomena again can be abandoned.

In order to illustrate some of the features of the precipitation process, the structure of a single, matrix crystal in which the particles have grown to a resolvable size will be considered. The microstructure of such a sample is shown by Fig. 1. The particles are not equiaxed but appear to be needle-like. Actually they are plates. These plates are not randomly oriented but are parallel to some family of matrix planes—the {111} planes in Al–Ag alloys and {100} planes in Al–Cu alloys. In addition, the crystallographic lattice of the precipitate in each particle has a definite orientation relative to that of the matrix. In Al–Ag alloys the basal plane of the hexagonal precipitate structure is parallel to the {111} matrix planes with the ⟨11·0⟩ directions of the precipitate particles parallel to corresponding ⟨110⟩ directions of the matrix crystal. The Laue pattern for a crystal of the as-quenched (supersaturated solid solution) alloy shown by Fig. 2A is supplemented by a pattern of sharp spots for all of the precipitate particles in the four explicit orientations as illustrated by Fig. 2B. Thus, the microscopic and X-ray diffraction data reveal that all of the precipitate particles within a single, matrix crystal of the Al–Ag

Fig. 1. Micrograph of aluminum–20 % silver alloy aged 25½ hr. at 387° C. × 1300. Resolved cross-sections of precipitate plates are aligned in four orientations relative to the matrix single crystal.

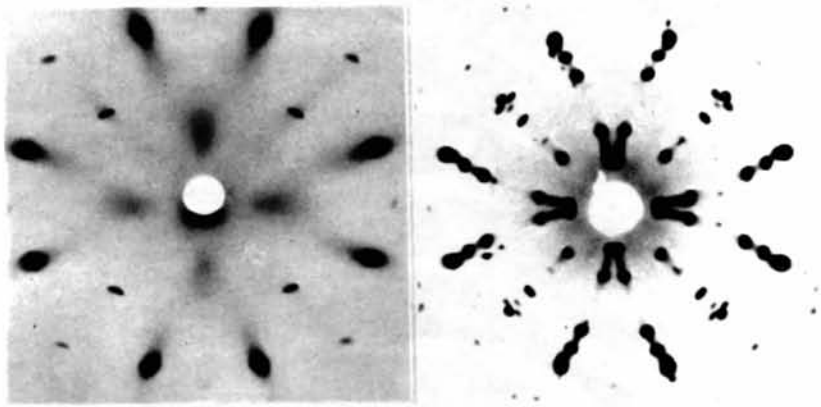

A B

Fig. 2. Laue patterns of Al–Ag alloy. [100] parallel to the beam. Co radiation. A, as-quenched—matrix spots only; B, aged 1 hr. at 320° C.—sharp matrix and precipitate spots.

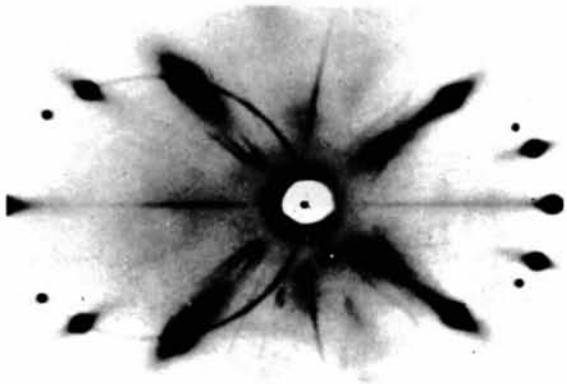

Fig. 3. Laue pattern of aged Al–Mg–Si alloy showing streaks produced by diffraction of white radiation from precipitate in platelet stage. Aged 1 hr. at 300° C. Cr radiation.

*To face p.* 238

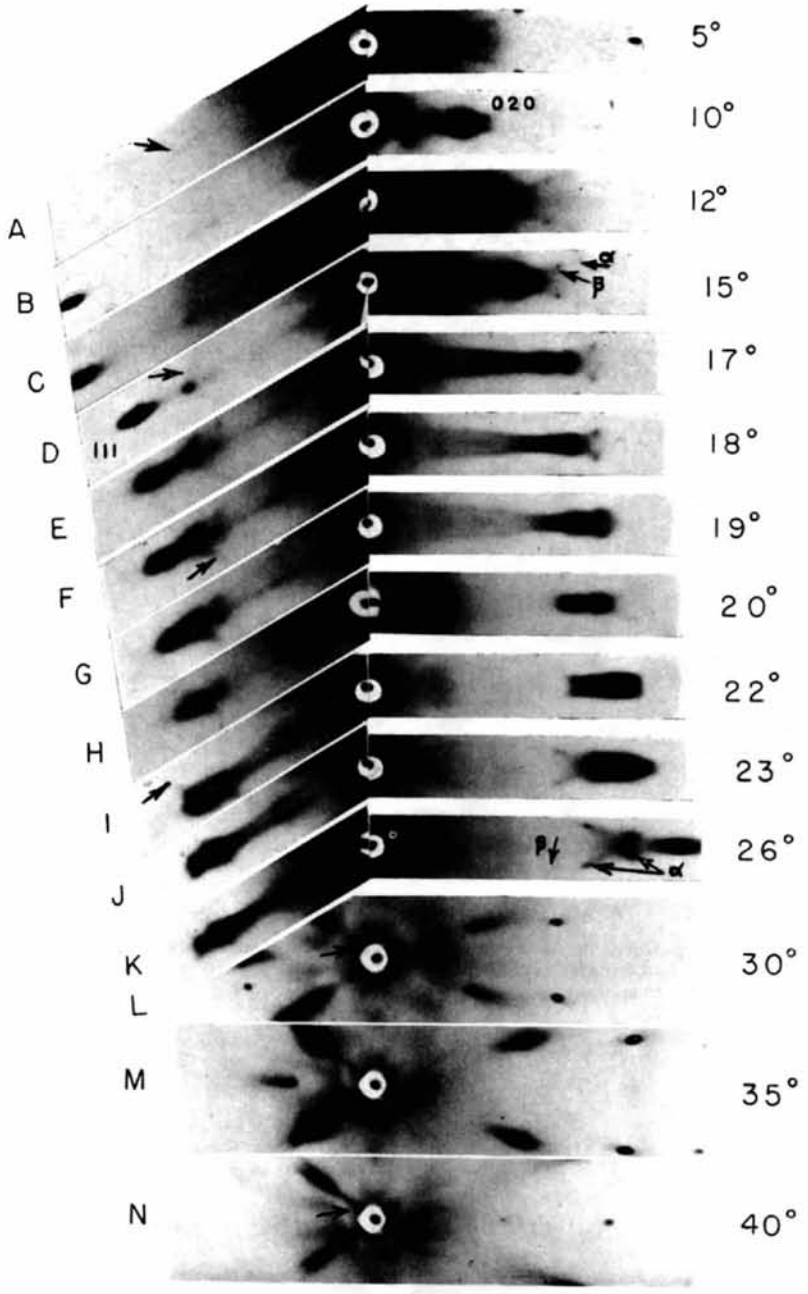


Fig. 4. Series of Laue patterns for aged Al–Ag alloy in which precipitate particles range from stringlets to platelets. Orientation of crystal given by angle between [100] and direct beam with [001] vertical. Cu radiation and flat film.

alloy fall into one of the four orientations in regard to both shape and crystallographic lattice.

Consider also that the precipitation process is governed by rates of nucleation and growth of the particles. The particles grow from only a few unit cells to sizes which depend upon the time and temperature of the precipitation or aging treatment.* At some stages during the course of growth one dimension of plate-like particles will be less than that required for sharp diffraction, while the lateral dimensions are adequate. Yet there are only the few distinct orientations in a single, matrix crystal. Here, then, is the ideal and perhaps a unique condition for studying the effects on the diffraction pattern of particle shape and size when some dimensions are below that required for sharp diffraction. The number of particles may be large to provide intense diffraction, but they are all accurately aligned in the few orientations. The condition is quite different from powder diffraction analyses of very small but randomly oriented particles in which particle shape is more difficult to distinguish in interpreting diffuse and low-angle scattering. Diffraction effects which are observed when the particles are smaller in one or more dimensions than that required for the sharp Laue spots of Fig. 2B will be considered in detail in this work.

## 2. Previous investigations

Studies of the diffraction patterns of aged alloys and their structural implications have been the subject of several papers in the past. In the early work of Calvet, Jacquet & Guinier (1939) in France and of Preston (1938*a*, *b*, 1940) in England on aluminum-base copper alloys, the patterns exhibited streaks which were attributed to two-dimensional gratings on the {100} planes of the parent crystal. The assumption was made that these gratings which developed during the early stage of aging were plate-like clusters of copper atoms with the same structure as the aluminum matrix. The technique used by Guinier in this and later work on Al–Cu (Guinier, 1946) and subsequent work on Cu–Be (Guinier & Jacquet, 1943, 1944), Al–Ag (Guinier, 1942, 1946) and Al–Zn (Guinier, 1943) alloys involved monochromated radiation with both stationary and oscillating crystal methods. On the other hand, Preston used the transmission Laue technique with general radiation. Similar diffraction phenomena have been observed in Laue patterns of Al–Ag (Barrett, Geisler & Mehl, 1941), Al–Zn (Geisler, Barrett & Mehl, 1943*b*), Al–Mg (Geisler *et al.* 1943*b*) alloys, but in these cases the orientations of the gratings varied with differences in crystal structure and Widmanstätten relations of the precipitating phase. The latter authors attributed the two-dimensional diffraction phenomena to very thin plate-like particles or 'platelets' of the precipitating structure which have the same lattice or one closely resembling that of the precipitate particles when they have grown thick enough to diffract as three-dimensional gratings. The work reported here discusses the advantages and limitations of the various techniques; it presents a method which has been quite successful and which is illustrated first by a somewhat simple structure (Al–Ag) and later by a complex structure (Al–Mg–Si); and finally it summarizes the interpretations of the diffraction phenomena.

## 3. Limitations of the various methods

For identification of the two- and one-dimensional diffraction effects, in which one or two of the Laue conditions are relaxed, single-crystal methods have been found most useful. Indeed, the quantity of second phase in even the fully grown condition may be too small in relation to the quantity of matrix to give a detectable pattern in photograms of powdered or polycrystalline aggregates. The Al–Mg–Si alloys which contained only 1·4 % alloying elements afforded a good example of this, since lines for any phase other than the aluminum matrix could not be detected in the powder pattern, whereas diffraction from the earliest stages onward to the usual $Mg_2Si$ structure was observed in patterns for single crystals, as will be described later. In this case, single-crystal techniques were essential.

For analyzing the diffraction effects observed in the early stages of precipitation one single-crystal technique consists of stereographically plotting the streaks which appear in Laue patterns (Geisler *et al.* 1943*b*; Barrett & Geisler, 1940; Guy, Barrett & Mehl, 1948). The streaks in patterns for Al–Mg and Al–Cu alloys coincide with great circles which are directed to the poles of a certain family of planes. Reciprocal-lattice plots can be constructed for those streaks which are associated with matrix Laue spots. The streaks are represented as rods in the reciprocal lattice, and these are along those crystallographic directions in which the indeterminate periodicity exists in the structure. The rods are along the ⟨100⟩ and ⟨111⟩ directions in Al–Cu and Al–Ag alloys, respectively, and these are the directions through the thickness dimensions of the plate-like precipitate particles in the two alloy systems.

Such an analysis, which depends upon the streaks passing through Laue spots, was found to be inadequate in analyzing the short streaks first found in patterns for Al–Mg alloys (Geisler *et al.* 1943*b*) and more recently observed in patterns for Al–Mg–Si alloys as in Fig. 3. The more prominent streaks of Fig. 3 which pass through Laue spots can be readily plotted as the zonal circles through {100} poles,* as in Fig. 5. The short streaks, however, cannot be plotted with sufficient accuracy to permit judicious directing of great

* It will be shown later that these streaks can originate from rods parallel to any directions of the form *hk*0, i.e. any platelets on {100}, {110}, {120}, or {130}, etc., will produce these streaks.

circles to poles of matrix planes. A slight misjudgement in measuring the azimuth angle of arbitrary points on the streaks can appreciably change the direction of the rods in the projection.

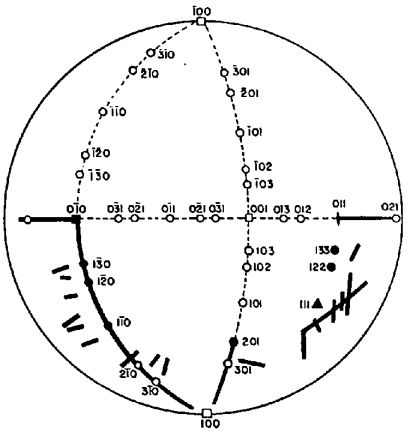

Fig. 5. Stereographic projection of pattern for Al–Mg–Si alloy aged 1 hr. at 300° C.

as in Fig. 6A, or by a range of $L$, as in Fig. 6B.* The latter construction in which the rods are projected parallel to themselves towards the origin has been found to be the more convenient in interpreting the white-radiation streaks. Such a construction is used in Fig. 7 to show that rods which do not pass through a matrix point as in Fig. 7A can produce streaks through Laue spots for the matrix as in Fig. 7C, so that the general interpretation of Fig. 7D is not always correct.† This ambiguity of white-radiation streaks arises when a rod is near to a matrix point and intersects the line from the origin through the matrix point. An example of such an ambiguity was illustrated by Figs. 3 and 5, in which the prominent {100} zonal streaks do not correspond to rods through (100) points. The rods are in the principal planes of the reciprocal lattice which contain {$hk0$} points, but the majority do not go through any matrix points.

The limitations of the white-radiation techniques are reduced by using one wave-length, either monochromatic radiation or the $K\alpha$ component of general radiation. Oscillating-crystal methods are useful in

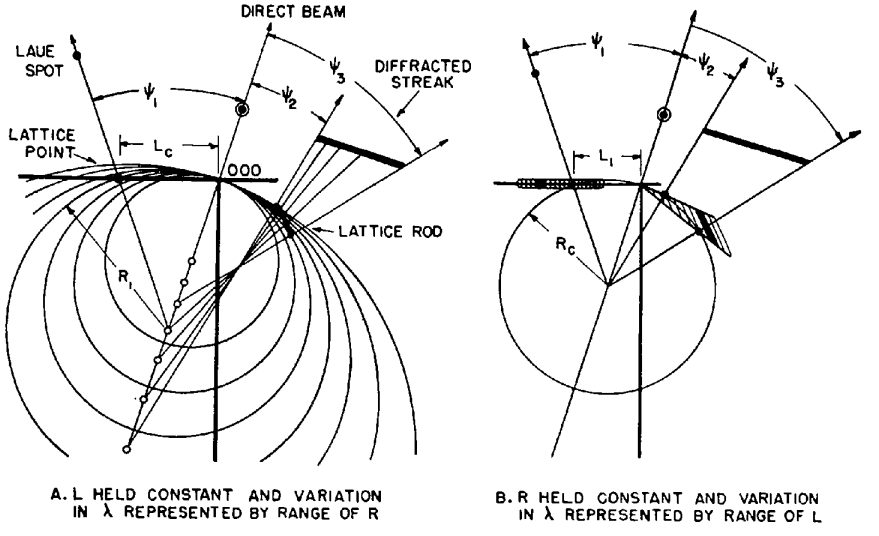


Fig. 6. Reciprocal-lattice construction for white radiation.

A further limitation of the stereographic plot can be illustrated by Figs. 6 and 7. These will show that streaks through matrix Laue spots may not correspond to rods through matrix points, as is generally assumed when analyzing white-radiation streaks. First, consider the reciprocal-lattice constructions for white radiation as in Fig. 6. The relation between interplanar spacing, $d_{hkl}$, and distance in the reciprocal lattice from (000) to the ($hkl$) point, $L$, can be represented as follows:

$$L=R\lambda/d_{hkl}, \qquad (1)$$

where the proportionality constant, $R\lambda$, is the product of the radius of the sphere of reflection, $R$, and the wave-length, $\lambda$. The range of wave-lengths in white radiation can be represented either by a range of $R$, locating the reciprocal-lattice rods when the diffraction effects are sufficiently intense; however, the diffraction effects in Fig. 3 were not detected in oscillating-crystal patterns made by the usual technique. In addition, one-dimensional diffraction effects, evidence for which

* The two modes of representation are related simply by the expression

$$L_c/R_1=L_1/R_c, \qquad (2)$$

where $R_1$ is the radius of the reflection sphere for the wave-length which diffracts from ($hkl$) at the fixed distance $L_c$ as in Fig. 6A, whereas $L_1$ is the apparent position of the point for diffraction when the sphere radius is constant ($R_c$) as in Fig. 6B.

† The rods are actually directed through matrix points in reciprocal-lattice constructions of Al–Cu and Al–Ag alloys, a consequence of the coherent growth of platelets in these alloys; however, coherent growth does not require all rods to pass through matrix points.

will be reported, are more difficult to detect with oscillating crystals than with stationary crystals. Thus, the trend is toward methods involving stationary crystals and characteristic radiation as the most powerful technique for studying the structures developed in the early stages of aging.

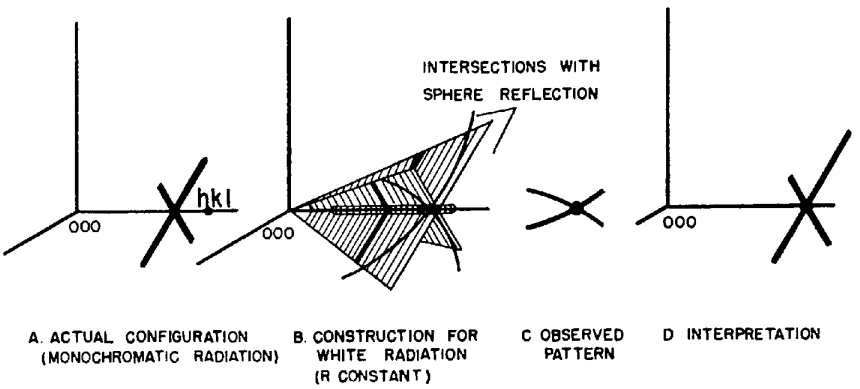


Fig. 7. An interpretation of streaks produced by white radiation.

### 4. Stationary crystal and characteristic radiation method

The method used in the present work consisted of making a series of patterns for a stationary matrix crystal at positions which were varied from one exposure to the next by 5° or less about a cube-axis. The characteristic components of general radiation were used.* General radiation of such a wave-length distribution that low background intensity existed adjacent to the $K\alpha$ peak was most suitable. Thus, the $K\alpha$ spots from the reciprocal-lattice rods were remote from the more intense portions of the white-radiation streaks. An intense source of monochromated radiation possibly would have been better, but this technique was found to be adequate. The scheme is illustrated by Fig. 8. Intersections of the sphere of reflection with the existing lattice rods were located from the platelet $K\alpha$ spots on the film for each position of the specimen. Corresponding points from one film to the next were connected to define the length, location and orientation of the rods in the reciprocal lattice. Sufficient data could be obtained on using a flat film and 5 cm. film-to-specimen distance to define most of the diffracting features within the (000) to (200) cube of the reciprocal lattice of the matrix.

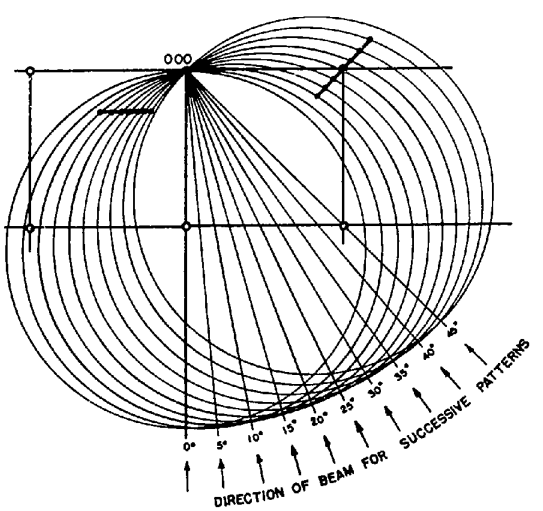


Fig. 8. Locating reciprocal-lattice rods.

### 5. Application to Al–Ag alloy

A portion of the series of patterns made for an aluminum-base 20% silver alloy crystal which had been aged about 8 years at room temperature is reproduced in Fig. 4. Unfiltered copper radiation was used. The Cu $K\alpha$ and $K\beta$ platelet spots are apparent near the (111) and (200) Laue spots. A few exposures were made using a nickel filter in order to identify the $K\beta$ spots,* but generally the filter was omitted in order to gain intensity in a reasonable exposure time (8 hr.). In addition, the $K\beta$ spots were analyzed and plotted to supplement the results for $K\alpha$. The corresponding $K\alpha$ and $K\beta$ platelet spots merge into the (111) and (200) matrix spots when these planes are diffracting $K\alpha$ and $K\beta$ wave-lengths respectively (Fig. 4G, H and I). Thus, the rods pass through reciprocal-lattice points of the (111) and (200) matrix planes.

The reciprocal lattice is the most convenient form for presenting and interpreting the data. The analysis of the film measurements is illustrated by Fig. 9. Coordinates of the spots on the film are measured as indicated for the spots $A'$ and $B'$. The horizontal coordinate, $X$, and the film-to-specimen distance, $D$, are used to calculate the angle, $\psi$, between the direct beam

* These features of the technique are not unlike those used to analyze preferred orientations and to obtain data for plotting pole figures of polycrystalline materials.

* The relative intensities of the $\alpha$ and $\beta$ spots are very deceiving, for apparently the intensity of scattering varies along the length of the rods, being greatest near the center and less at the ends. Spots for $\beta$ intersections near the center of the rods have been observed to be more intense than spots on the same pattern for $\alpha$ intersections near the ends of the rods, as illustrated near the (200) Laue spot in Fig. 4D and E.

and the diffracted beam projected on to the horizontal plane according to expression (3) in the legend of Fig. 9. Likewise, both film co-ordinates and the arbitrary radius, $R$, are used in (4) to calculate the projected distance, $r$, from the center of the sphere of reflection to the reciprocal-lattice point. Finally, the vertical co-ordinate in the reciprocal lattice, $\zeta$, may be calculated from (5). The construction in Fig. 9, which shows the diffracted beams parallel to lines from the center of the sphere of reflection to the lattice points, is easily verified for normal Bragg diffraction (Barrett, 1943, p. 104). It is the basis of the most convenient method of plotting the data for the reciprocal-lattice rods and proved to be suitable also for these cases of diffraction in which one of the Laue conditions was relaxed.

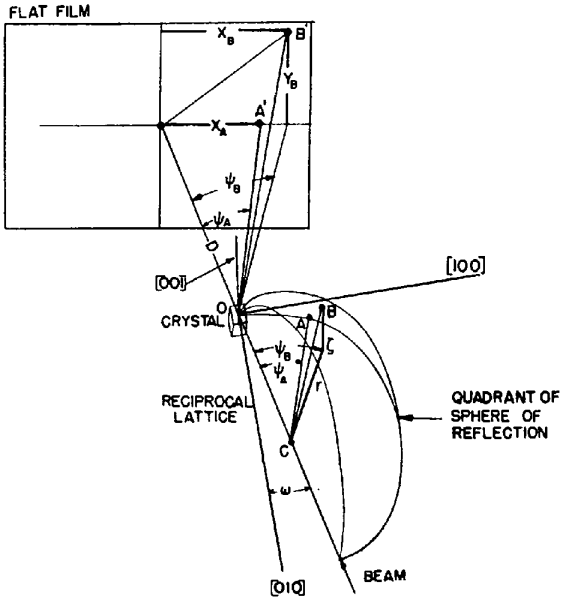


Fig. 9. Analysis of film measurements.

$$\psi = \tan^{-1}(X/D), \tag{3}$$

$$R = OC = CA = CB,$$

$$r = R\sqrt{(D^2+X^2)}/\sqrt{(D^2+X^2+Y^2)}, \tag{4}$$

$$\zeta = \sqrt{(R^2-r^2)}. \tag{5}$$

A convenient method of plotting a projection of the data on to the principal horizontal plane of the reciprocal lattice is illustrated by Fig. 10. A plotting device was designed which consists of two arms and two protractors. One protractor is fixed at the origin of the reciprocal-lattice plot, and arm 1, which represents the direct beam, is pivoted here. This protractor is used to set arm 1 at the angle between the direct beam and some prominent crystallographic direction in the crystal, $\omega$, set in making the particular pattern (compare Figs. 9 and 10). The length of arm 1 is equivalent to the arbitrary radius of the reflection sphere (20 cm. was used). The other end of this arm bears a 360° protractor centered at the point which represents the center of the sphere of reflection. This point then is the pivot for the second arm, and the angle $\psi$ between the two arms can be set on the 360° protractor. The other end of arm 2, which represents the diffracted beam direction, carries a pencil point and clamp arrangement whereby the effective length of the arm can be varied with changes in $r$. The reciprocal point is plotted with the pencil by setting $r$, $\psi$ and $\omega$. The device considerably simplified the plotting of the reciprocal-lattice rods and was also useful in plotting lattice points for Bragg diffraction from oscillating crystal patterns. In this case, the limits of position of a reciprocal point were scribed on the plot by moving arm 1 over the range of oscillation on the protractor at the origin (i.e. from $\omega_1$ to $\omega_2$ when the diffraction was observed to occur somewhere between these positions). For a cylindrical film the relations

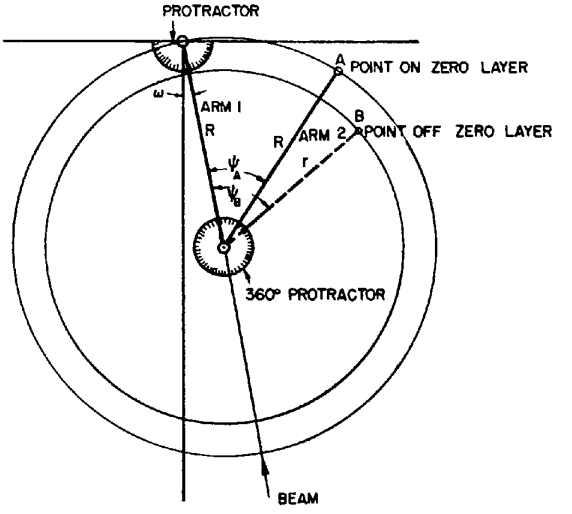


Fig. 10. Plotting data in reciprocal lattice.

between film co-ordinates, radius of film, $R_f$, radius of reflection sphere, $R_s$, and the quantities used for plotting the reciprocal points are as follows:

$$\psi = 360X/2\pi R_f, \tag{6}$$

$$r = R_f R_s/\sqrt{(R_f^2+Y^2)}, \tag{7}$$

$$\zeta = YR_s/\sqrt{(R_f^2+Y^2)} = \sqrt{(R_s^2-r^2)}. \tag{8}$$

For a constant value of film radius, added convenience is obtained by calibrating the 360° protractor in terms of the $X$ film co-ordinate, and the scale on arm 2 for $r$ in terms of $Y$ co-ordinates, for then points may be plotted directly from film measurements. Accuracy comparable to that of the compass method and greater than that of Bernal charts can be achieved by this method. The use of a standard reflection-sphere radius inherent in the plotting device is not generally a disadvantage in analyzing crystal structures of different cell sizes or in using radiations of different wave-lengths, since the interplanar spacing is easily calculated from the reciprocal-lattice distances, $L$, by expression (1).

In regard to the analysis of the aged Al–Ag alloy, a portion of the reciprocal lattice which was determined and plotted from the series of patterns in Fig. 4 is shown by Fig. 11. The observed rods about (111) and (020) are plotted as double lines. These were parallel to the lines from (000) to the four (111) points and intersected in groups of four very near, or at, the (111) and (200) points. For reference, the points for thick particles of the hexagonal $\gamma'$ precipitate structure (Barrett *et al.* 1941) in the four orientations designated by letters are also plotted. The $\gamma'$ points appear on planes

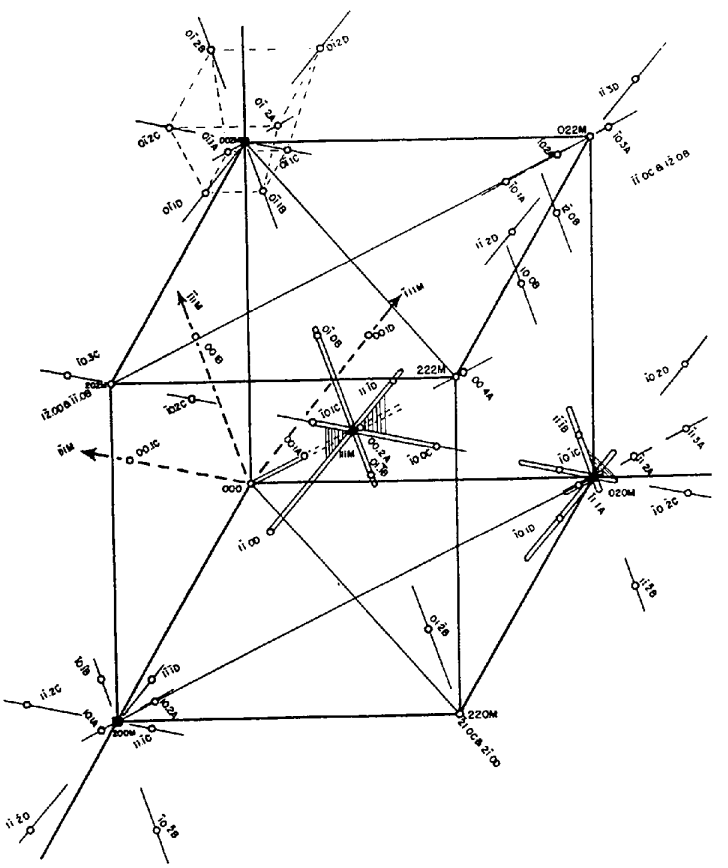

Fig. 11. Portion of reciprocal lattice for aged Al–Ag crystal.

in the reciprocal lattice which are parallel to {110} planes of the matrix crystal (defined by diagonals of horizontal faces of Fig. 11), and which are spaced at a distance equal to the (110) matrix reciprocal distance. This evolves from the fact that the atomic spacings on the (00.1) plane of $\gamma'$ are the same as those on the (111) plane of the matrix and the (11.0) plane spacing in $\gamma'$ is the same as the (220) spacing in the matrix. The structures are coherent on the conjugate planes. As a consequence of this all $\gamma'$ points are in line with matrix points in one of the four ⟨111⟩ directions.

The rods pass through matrix points, but they also pass through subsequent points for the precipitate when it has grown to a size conducive to normal Bragg diffraction. Thus, the interpretation is at first confused: do the rods represent an indefinite periodicity in the matrix {111} planes, or in the (00.1) plane of the precipitate in the four orientations? The latter is favored, and while a more complete discussion of interpretation will follow, evidence supporting this in Fig. 11 should be indicated at this time. First, the rods do not extend comparable distances on both sides of the matrix points, but their extent appears to be controlled by the subsequent positions of $\gamma'$ points. Near the (020$M$) point they are centered near $\gamma'$ points, while near the (111$M$) point they extend to, or slightly beyond, $\gamma'$ points about (111$M$). Secondly, rods parallel to the direction from (000) to (00.1$B$) pass through points for $\gamma'$ crystallites in the $B$ orientation, etc.* If, for example, a point for $\gamma'$ in the $D$ orientation had been on this rod, then a lack of periodicity in the matrix would be the only explanation; but this was not the case. There is only one rod through each

* The expected directions of the rods through other $\gamma'$ points are shown in Fig. 11 by short single lines. These are outside the volume which was investigated by using flat film. The use of cylindrical film would have extended the investigated volume of the reciprocal lattice.

potential $\gamma'$ point, and this rod is always parallel to the $\langle 00.1 \rangle$ direction of the $\gamma'$ crystallite responsible for the potential $\gamma'$ point. Thus, the subsequent presence of $\gamma'$ points influences the geometry of the rods, suggesting that plate-like particles of $\gamma'$ are present at this stage of aging, but these are too thin in the [00.1] direction to reveal definitely their structure.

The rod through (00.1$A$) and (00.2$A$) points could not be detected in the neighborhood of the (111) point, since diffraction for it is superimposed on the (111) Laue spot as explained by the construction in Fig. 12. This is inherent in the method, for any rod which is directed towards the origin and through, or towards, a matrix point will appear as a spot (regardless of wave-length) which will be superimposed on the matrix Laue spot. The rod could be detected at high angles only by using monochromatic radiation. On the other hand, the presence of a rod in this direction but at

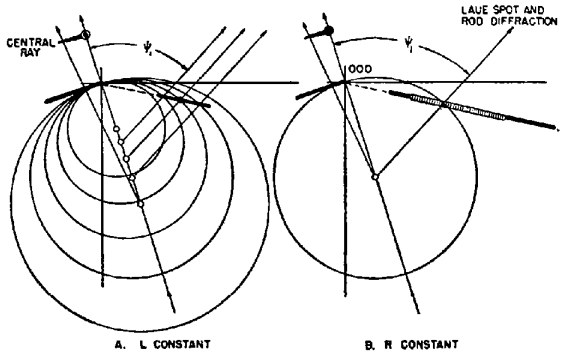


Fig. 12. Diffraction for rods directed towards origin in line with matrix point superimposed on Laue spot when general radiation is used. Rods at (000) produce central rays in patterns regardless of wave-length.

(000) is verified by examining the low-angle regions of certain patterns. When the reflection spheres are tangent, or nearly tangent, to these rods, as illustrated at the left portions of the two diagrams in Fig. 12, short streaks extend out from the central beam as in Fig. 4L to 4N. These appear regardless of wave-length, whether white or monochromatic, and are the principal contributors to the low-angle scattering which has been observed with polycrystalline specimens of aged alloys (Guinier, 1942, 1943, 1946; Guinier & Jacquet, 1943, 1944). The geometry of the central rays furnishes an immediate clue to the direction of the rods. With Al–Ag crystals the rays appear when the beam is directed along a [110] direction, and they extend in the four $\langle 111 \rangle$ directions; at this orientation the reflection sphere is tangent to the plane which contains four rods through (000). With Al–Cu (Preston, 1938*a*, *b*, 1940; Barrett & Geisler, 1940), and Cu–Be (Guy *et al.* 1948) crystals, in which the platelets form on {100} planes, central rays are observed to extend in the [001] and [010] directions when [100] is parallel to the beam and in the [001] direction when [110] is parallel to the beam. Again at these orientations the reflection sphere is tangent to the corresponding lattice rods at (000).

The presence of rods in the reciprocal lattice has not been adequate to explain fully all diffraction phenomena that have been observed with the more extensively investigated alloys. The first instance of this was the diffraction effect that resembled a doubled cross (Barrett & Geisler, 1940). This appeared near the center of patterns of Al–Ag crystals aligned with [100] parallel to the beam at a very early stage of aging (Fig. 13A) and diminished in intensity when the platelet streaks were most intensely developed (Fig. 13D). Originally the doubled cross was ascribed to the blending of several white radiation streaks that corresponded to rods through (120) and ($\bar{1}$20) points, but more recently it was shown that this configuration also appeared on patterns made with monochromatic radiation (Guinier, personal communication). Thus, this diffraction phenomena must be caused by a planar diffraction configuration adjacent to the origin of the reciprocal lattice.* Such a configuration, which adequately explains the doubled cross as well as similar streaks in the small-angle portions of patterns for other orientations (Figs. 13B, C), is illustrated by Fig. 17. Here the (00.2)-type rods have been connected together by the shaded planes. These are intended to illustrate only the orientations of the areas of diffraction and not necessarily their boundaries. The intensity of diffraction is greatest at the rods, and it tapers off in the planes on both sides of the rods. Those reciprocal planes of Fig. 17 responsible for the various central streaks are inscribed on some of the patterns of Fig. 13.

While the diffraction at (000) is independent of wave-length and is most intense here, planar diffraction areas of the type shown by Fig. 17 were observed at other regions of the reciprocal lattice also. These were indicated by streaks for $K\alpha$ and $K\beta$ wave-length (in contrast to spots for rods). The presence of such planes is demonstrated by the vertical bridge of the Cu $K$ platelet spots near the (111) spot in Fig. 4D–F, and by the diagonal $K\alpha$ bridges between the spots near (200) in Fig. 4J and K. These features are represented by the small shaded planes in Fig. 11. All six orientations of the planes of Fig. 17 were not detected in the vicinity of (111) and (020) matrix spots. This can easily be explained on the basis of a construction similar to Fig. 12. Diffraction for planes directed towards the origin falls on the white radiation streaks for some of the rods, while that for other planes may be confused with $K$ streaks for rods that are tangent to the re-

* This is perhaps the first evidence for one-dimensional X-ray diffraction that has ever been identified; neither white radiation nor near-tangency of the reflection sphere with central rods can account for it. Individual features can be followed over a large range of specimen orientation, thus suggesting planar areas in the reciprocal lattice. Finally, it is associated with growth of precipitate particles.

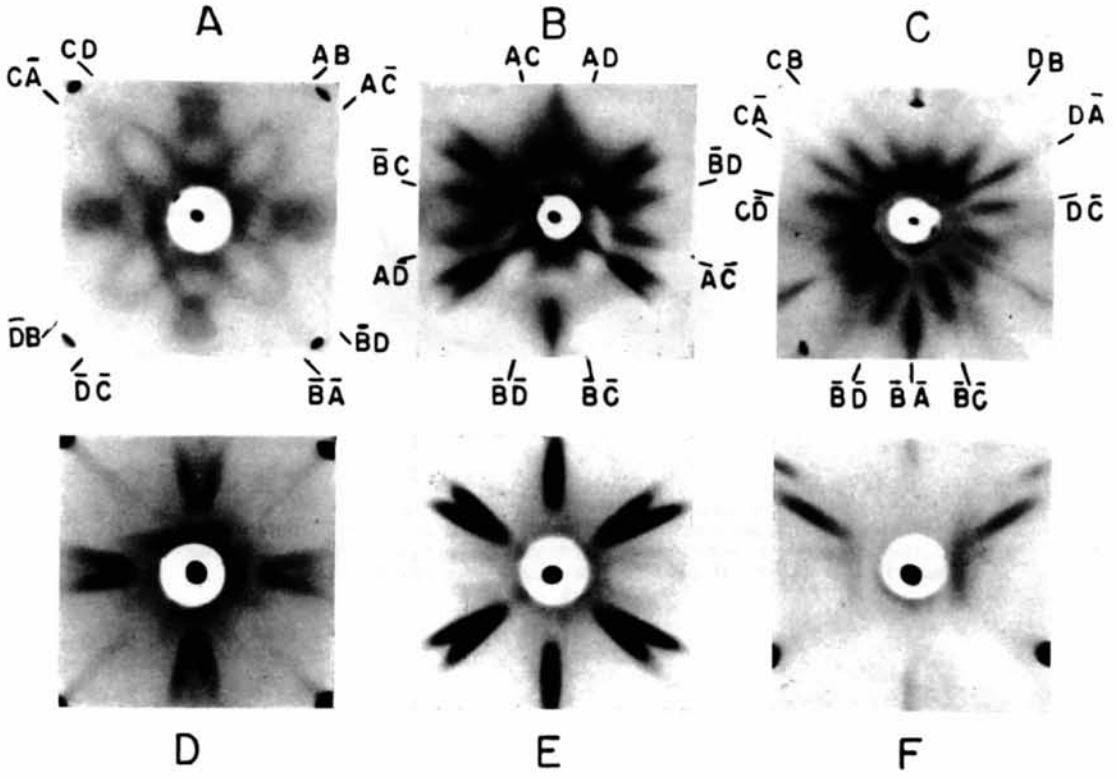


Fig. 13. Central portion of patterns of aged Al–Ag alloy. A, B and C, platelet and stringlet stage. Aged at room temperature. D, E and F, platelet stage more prominent. Aged 104 hr. at 150° C. Intense streaks are caused by white radiation and rods. A and D, [100] parallel to beam; B and E, [110] parallel to beam; C and F, [111] parallel to beam.

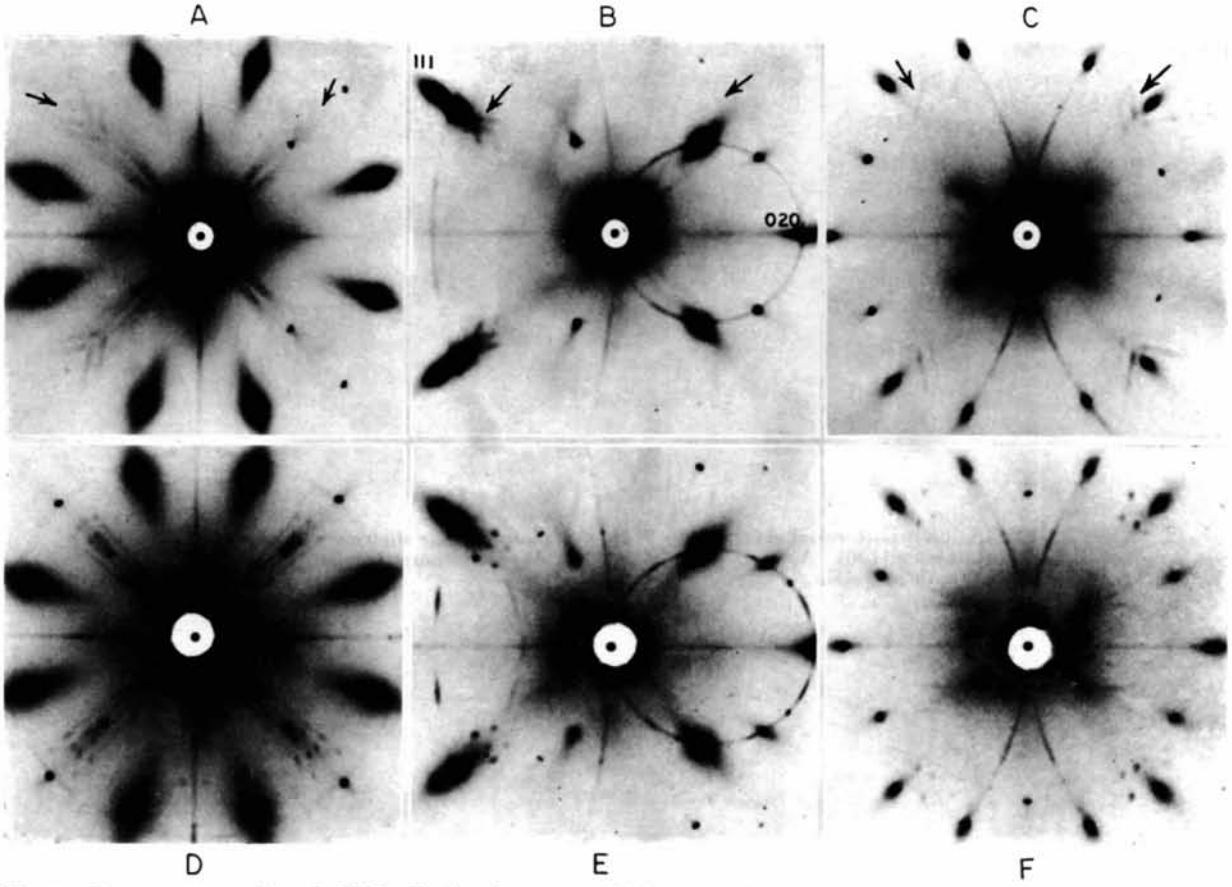


Fig. 14. Laue patterns of aged Al–Mg–Si alloy in stages which are predominantly stringlet (A, B and C) and platelet (D, E and F). Cu radiation. A, B and C, aged 4 hr. at 220° C.; D, E and F, aged ½ hr. at 300° C.; A and D, [100] parallel to beam and [001] vertical; B and E, rotated 20° about [001]. C and F, [110] parallel to beam.

*To face p. 244*

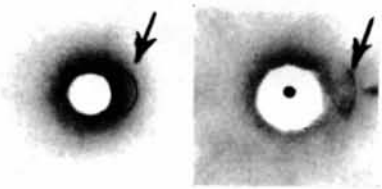

A B

Fig. 15. Central area of Laue patterns for aged Al–Mg–Si alloy. Crystals set about 5° from [100] parallel to the beam. Ellipse at very low angles in A indicates a planar area at (000) defined by [001] and [010]. This resolves on further aging into rods as revealed by low-angle spots in B. A, stringlet stage—aged 4 hr. at 220° C.; B, platelet stage—aged ¼ hr. at 300° C.

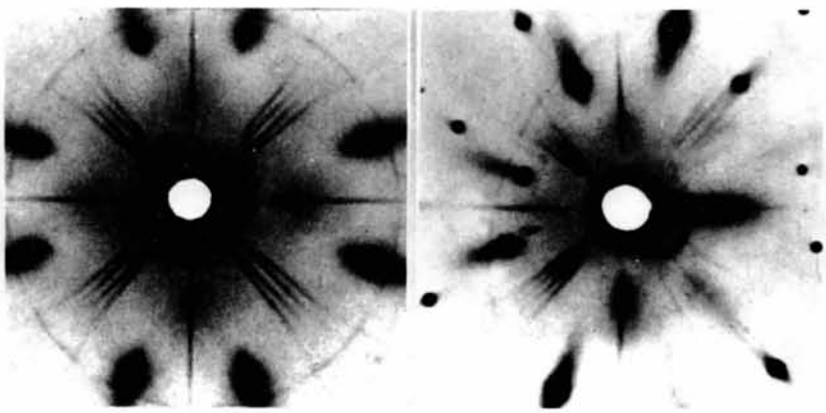

A B

Fig. 16. Laue patterns of aged Al–Mg–Si alloy at platelet stage showing concentric circle about [100]. A, aged ½ hr. at 300° C., Mo radiation; B, aged 3 hr. at 300° C., Cr radiation.

flection sphere. Nevertheless, sufficient data were observed to show that the rods are not uniformly diffuse in cross-section at the earlier stage, but that they develop from planar areas which appear in the

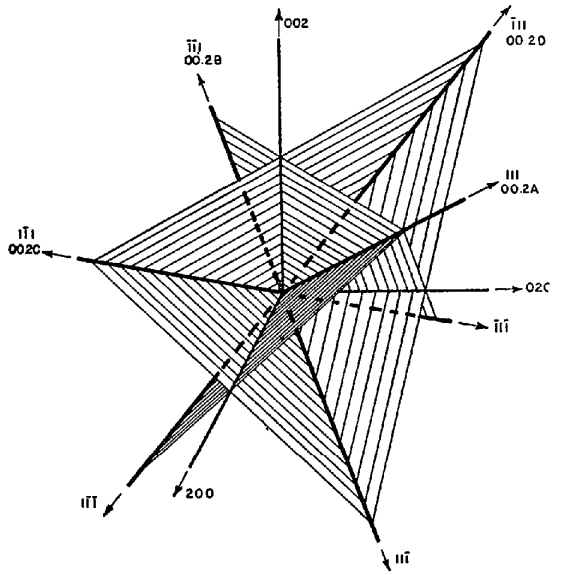


Fig. 17. Region of diffraction about (000) reciprocal-lattice point of aged Al–Ag crystal.

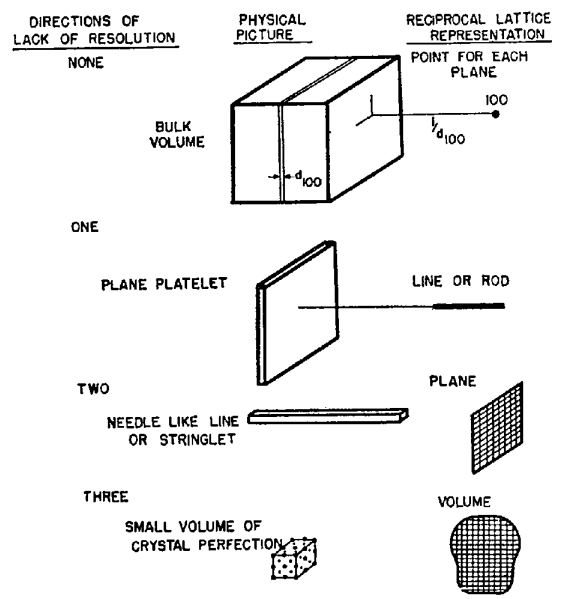


Fig. 18. Relations between physical geometry of small crystals and reciprocal-lattice representation.

reciprocal lattice perpendicular to the ⟨110⟩ direction of the matrix crystal.

An interpretation of the small plane areas of diffraction observed in the reciprocal lattice of Al–Ag (and later Al–Mg–Si) should now be made in order that a convenient name can be applied to the physical structure considered responsible for these diffraction effects. By analogy with other types of space transforms illustrated by Fig. 18, the reciprocal plane represents a two-dimensional indefiniteness of periodicity, relaxation of Laue conditions, or simply lack of resolution. The term 'platelet' has been used to refer to the structure which produces the diffraction effects that are represented by rods. The space transform of thin crystal plates can be approximated by short lines or rods perpendicular to the plane of the plate through the normal points for Bragg diffraction (Ewald, 1940). Thus, by analogy, the term 'stringlet' will be used for convenience in discussing the predominantly one-dimensional structure which accounts for the small planes in the reciprocal lattice of an aged alloy.

### 6. Structure of aged Al–Mg–Si alloy

The structure of an Al–Mg–Si alloy could be conveniently studied at all stages of aging by single-crystal techniques. The alloy, which contained Mg and Si equivalent to 1·4% magnesium silicide, had been used for an earlier investigation in the field of electron microscopy (Geisler & Keller, 1947). When precipitation is complete, as provided by high-temperature aging, the precipitate has the normal structure of the equilibrium second phase, $Mg_2Si$—that is, face-centered cubic structure of the $CaF_2$ type with $a_0 = 6{\cdot}39$ A. Oscillating crystal patterns of a fully aged sample verified this and also provided the following orientation relationships between the particles of $Mg_2Si$ and the aluminum matrix crystal:

$$(100)Mg_2Si \parallel (100)Al, \quad [110]Mg_2Si \parallel [100]Al.$$

The $Mg_2Si$ particles generally appear as plates parallel to {100} planes of the matrix (Geisler & Keller, 1947); however, plates sometimes also appear parallel to {110} planes (Mehl, Barrett & Rhines, 1932). While these crystallographic considerations are quite important in interpreting the mechanism of the precipitation processes, the intermediate structures are those which are interesting to the crystallographer from the standpoint of structure analysis and to the metallurgist from the standpoint of age-hardening theory.

#### (*a*) *The stringlet stage*

The analysis described in a previous part of the paper was developed for determination of the structures diffracting in the early stages of aging of this alloy when the stereographic plot of white radiation streaks was found inadequate. Crystals corresponding to two aging conditions were analyzed: one at which the stringlet structure was well developed, and the other at which the platelet structure was well developed. Three patterns from each of the series of sixteen (varying in crystal orientation by 2 to 5°) are reproduced in Fig. 14. The short, approximately horizontal and vertical $K\alpha$ and $K\beta$ streaks at the diagonal positions in pattern A, those to the right of center in pattern B and those at the diagonal positions in

pattern C define the three sets of planes of the type in the diagram of Fig. 19. Those in the left part of pattern B near the (111) Laue spot define the planes near the (111) matrix point in the reciprocal lattice of Fig. 19. Although the latter areas are near the (111) matrix point and might remotely be attributed to a lack of periodicity in the matrix structure, the former areas are near but detectably removed from a (110)-type point (this is not a reflection for the face-centered cubic matrix). Since the stringlet areas in the

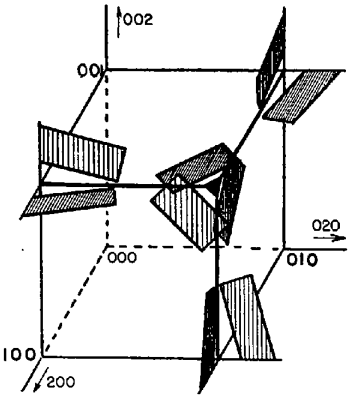


Fig. 19. Reflection areas near (110) Al and (111) Al points in reciprocal lattice for Al–Mg–Si alloy produced by the precipitate in the stringlet stage. Alloy aged 4 hr. at 220° C.

reciprocal lattice are perpendicular to ⟨100⟩ directions of the crystal, the resolvable directions of the stringlets are along the cube edges of the matrix. As shown in Fig. 19, the stringlet diffraction areas are in planes through the reciprocal lattice parallel to the principal (cubic) planes of the matrix lattice and intersecting the three axes at distances equal to the lattice parameter of the matrix crystal. As the growth of the structure progresses, this condition persists, suggesting that some dimensions of the precipitate are the same as that of the matrix. This is evidence for a coherent transition structure as illustrated for Al–Ag by Fig. 11.

### (*b*) *The platelet stage*

Comparison of corresponding patterns in Fig. 14 shows that $\alpha$ and $\beta$ platelet spots evolve directly from the $\alpha$ and $\beta$ stringlet streaks. The structure of the stringlet has developed to the point where there is an indefiniteness in one direction only. Reciprocal-lattice projections of the data for the platelet rods are given in Fig. 20. Most of the data were on the 0 layers (the principal planes), in $K\alpha$ and $K\beta$ planes at the (001) Al distance, or represented inclined rods in $K\alpha$ and $K\beta$ planes at (100) and (010) distances.* The manner in which these planes fitted together in space to form a portion of the one quadrant of the reciprocal lattice is illustrated by Fig. 21. Comparison of Figs. 20 and 21 with Fig. 19 suggests that the platelet rods evolve from the stringlet planes by the disappearance of central portions of the planes to leave certain of the edges as rods. These edges also shrink slightly on becoming rods, showing that the resolution in the least definite direction (the particle thickness) has increased somewhat. The rods are generally unrelated to the matrix points in contrast to the structure of Al–Ag alloys (Fig. 11). They are more numerous and indicate platelets on more than one family of planes; judging from the directions of the rods the platelets are on {100} and {110} planes and possibly also {120}, {130} or {140} planes. They are also unrelated to the points for $Mg_2Si$ crystals in the three orientations, as shown by the small circles in Fig. 20.

Before discussing some of the other features of the patterns for Al–Mg–Si a brief description of the next stage of evolution should be considered. A series of oscillating-crystal patterns was made for a crystal which had been aged until Laue spots for the precipitate first appeared. It was found that the precipitate had a structure different from that of the usual form of $Mg_2Si$. Since the more prominent layer line (with [001] of the matrix as axis of oscillation) coincided with the first layer line of the aluminum matrix, the new structure is a transition lattice of the coherent type as observed in Al–Cu and Al–Ag alloys. The determination of its structure will appear in a future paper. It is sufficient here merely to show that it evolves directly from the platelet stage. A portion of the layer at an identity distance of about 4·1 A. ($d_{(001)\,Al}$) is illustrated by Fig. 22. The arcs shown are not platelet rods but represent the possible range of positions of the points for the transition structure, since a finite range of oscillation was used in locating the points. Comparison with Fig. 20C shows that each of the points develops by a shrinking of the platelet rods. The points lie quite accurately at the centers of the rods on the plane at $I = 4{\cdot}1$ A. with the exception of the two more distant points on the diagonal of Fig. 22. These may account either for inclined rods or for rods directed towards the (001) matrix point of Fig. 20C. Any rods of the latter type which may be tangent to the reflection sphere as the series of patterns is made may be completely missed or detected on only one pattern, as may be visualized by consulting Fig. 8. Indeed, several isolated spots were observed during the analysis of the patterns for the platelet stage. Thus, in this more complex structure the early diffraction effects can be traced directly to the transition lattice only, and to its corresponding reciprocal-lattice points, in a more satisfying degree than for the Al–Ag alloy (Fig. 11).

### (*c*) *Other features of* Al–Mg–Si *patterns*

Returning to the platelet stage, some of the diffraction effects caused by white radiation are somewhat unusual, but can be adequately explained on the basis

* Now that $K\alpha$ and $K\beta$ have been distinguished a few minor discrepancies are apparent on comparing Fig. 20B and C. Corresponding reflections for each rod should agree.

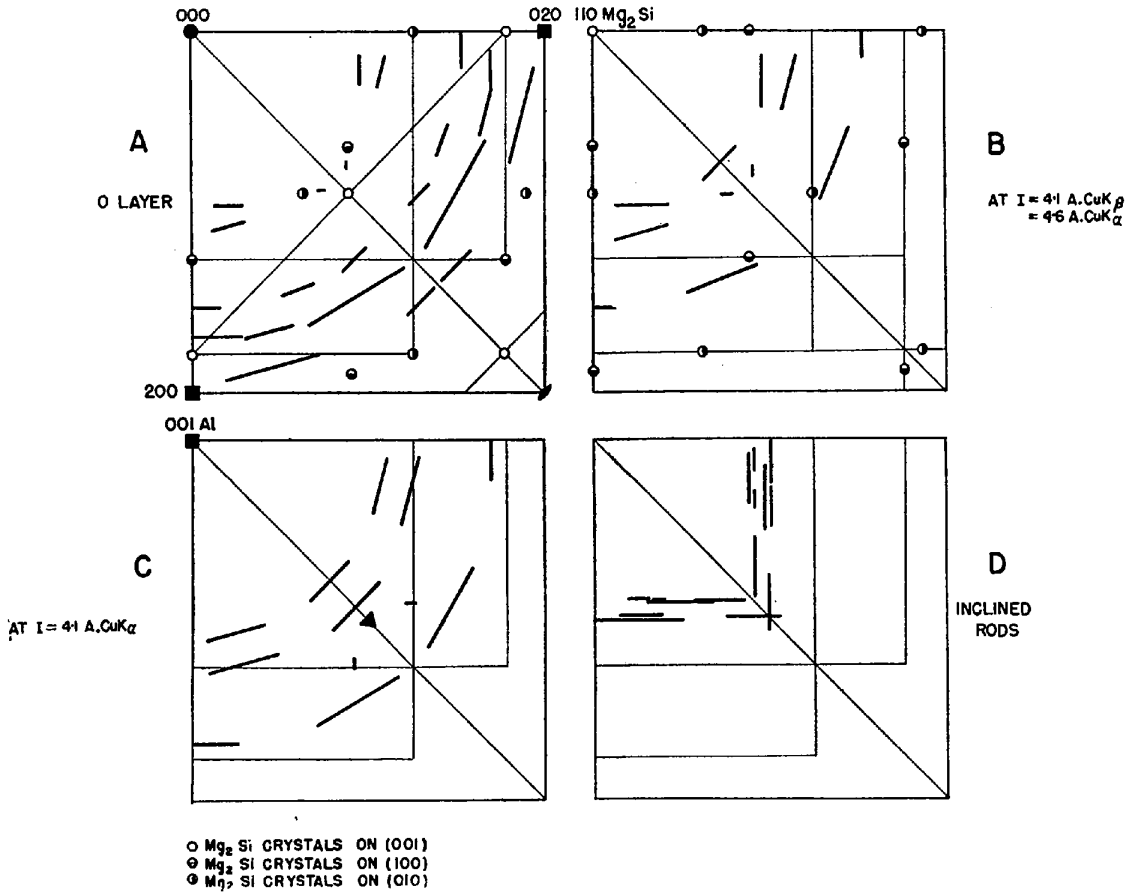


Fig. 20. Position of rods in reciprocal lattice of Al–Mg–Si alloy aged $\frac{1}{2}$ hr. at 300° C. Rods plotted for both $\alpha$ and $\beta$ Cu $K$ radiation. Matrix cell and subsequent $Mg_2Si$ points plotted for Cu $K\alpha$. $I$ is the identity distance to the first layer along cube directions of the matrix.

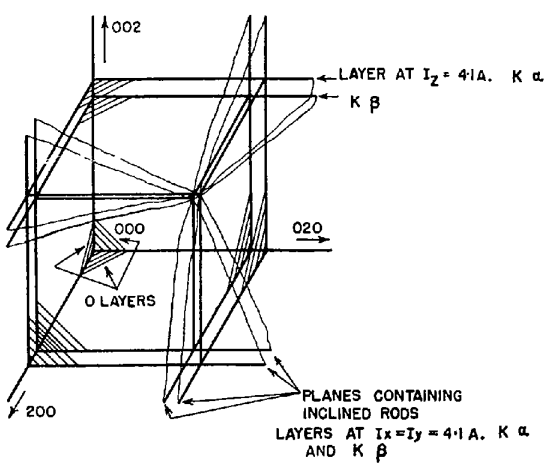


Fig. 21. Location of planes which contain rods in reciprocal lattice of Al–Mg–Si alloy.

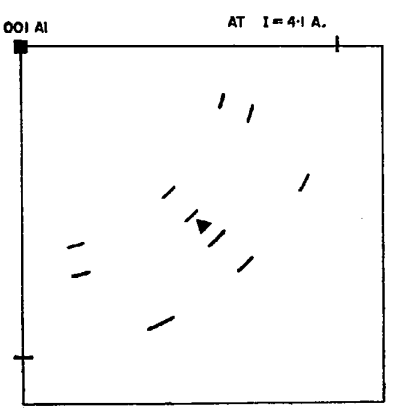


Fig. 22. Approximate positions of reciprocal-lattice points for transition structure observed in oscillating crystal patterns for Al–Mg–Si alloy aged 3 hr. at 300° C. Plane at $I = d_{(001)\,Al}$ shown only.

of the reciprocal lattice of Fig. 20. Consider first the {100}-type zonal streaks of Figs. 3 and 5. These consist of the prominent horizontal streak, the complete ellipse observed when the crystal is oriented at positions with the [100] direction 10–30° from the beam, and the predominantly vertical streak; these all pass through the direct beam as in Fig. 14. They can be attributed to either platelet rods or stringlet planes that lie in the principal planes of the reciprocal lattice (zero layers of Figs. 20 and 21). The shifting of the many rods or planar areas along these planes towards the origin to account for different wave-lengths (Fig. 6) in effect produces three complete planes of reflection. When the reflection sphere cuts the vertical plane (10–30° from perpendicular to beam) the complete ellipse which passes through the direct beam is diffracted. In a like manner the other vertical principal plane (10–30° from parallel to beam) accounts for the predominantly vertical zonal streaks.* The horizontal streaks then evolve from any reflection configuration in the horizontal plane containing the direct beam. If the sphere of reflection cuts any of the rods plotted for $\alpha$ or $\beta$ wave-lengths, then spots are superimposed on the streaks. Such spots on the {100} zonal streaks were used for plotting the rods in the zero layer. Obviously this family of zonal streaks produced by white radiation can originate from platelets on any planes of the form {$hk0$} and from stringlets along ⟨100⟩ directions; they were the most intense white-radiation streaks and were the first detectable evidence of structure change during aging.

The low-angle diffraction was rather general and diffuse, particularly when the beam was along a [100] direction of the aged Al–Mg–Si alloy. This would be expected since the reflection sphere is tangent to a stringlet plane area at (000) and is also tangent to the numerous rods which extend from (000). The presence of stringlet planes through (000) was confirmed. A small circle of the type explained above (Fig. 14B), but well within the minimum wave-length limit for diffraction configurations at locations other than (000), was observed when the sample was oriented with the [100] direction about 5° from the beam as in Fig. 15A. This corresponds to a stringlet reciprocal area at (000) in a vertical plane of the reciprocal lattice. At a later stage of aging (Fig. 15B) the circle contained $K\alpha$ spots for central rods.

A second prominent configuration produced by white radiation and characteristic of the platelet stage only (in contrast with [100] zonal streaks) is the concentric circle which appears about the direct beam when it is along a [100] direction, as in Fig. 14D. The concentric circle is not present at the stringlet stage (Fig. 14A); it appears at the same position in patterns made with Cu, Co, Cr, Ag or Mo (Fig. 16A) radiation, and its symmetry depends upon the orientation of the specimen, as may be seen by comparing Fig. 16A and B. Thus it is not a Debye circle. Close examination will show that it is not a continuous circle but consists of two types of arcs which are tangent to lines at 45° and at about 15° to the [001] and [010] directions. Examination of the plane at $I=4{\cdot}1$ A. of the reciprocal lattice of the platelet stage in Fig. 20C shows that there are rods at these angles. When these are projected in line with the origin to represent white radiation, they simulate planes which cut the sphere of reflection and produce the diffracted arcs, as illustrated by Fig. 23. When X-rays of higher energies are used

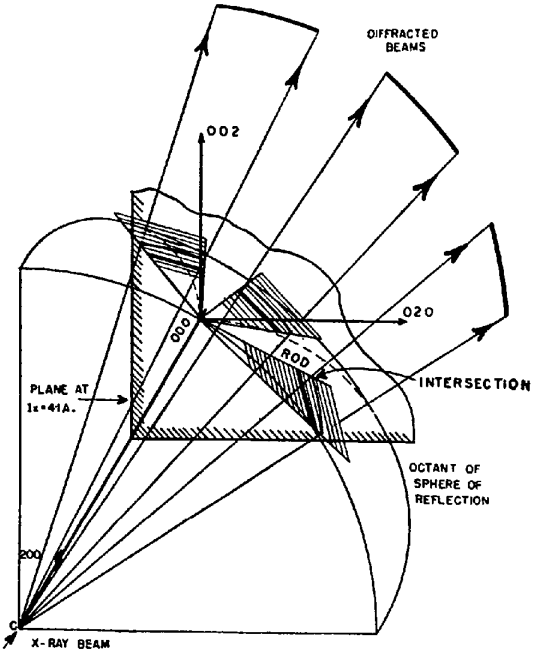


Fig. 23. Explanation of concentric circle.

the short wave-length limit is reduced and concentric diffraction effects from rods further from the (001) Al pole in Fig. 20C would be expected. Indeed, when Ag radiation at a peak voltage of 45 kV. was used, the concentric circle observed with Cu and Mo radiation (25 kV.) was supplemented by a circle closer to the center which agreed with the rod configuration most distant from (001) Al in Fig. 20C.

The arcs of the concentric circle are useful in verifying the rod construction; they confirm the observation that rods are present at angles of 0, 15 and 45° to ⟨100⟩ directions. Since the arcs are formed by the diffraction of practically a single wave-length, their lengths are a direct measure of the lengths of the rods in the reciprocal lattice. This is likewise a measure of the thickness of the platelet. The arcs of the concentric circle become shorter as aging is continued and the platelets grow thicker.

* When the two vertical planes make equal angles with the beam, i.e. [110] is parallel to the beam, the pair of streaks are symmetrical about the vertical as in Fig. 14C and F.

### 7. Interpretation of the diffraction phenomena

In the past there have been two opposing interpretations of the origin of diffuse diffraction from aged alloys. Both attribute it to an indefinite periodicity in certain crystallographic directions, but the one interpretation associates it with the matrix structure and the other with the precipitate structure. Features in the matrix structure which could produce such diffraction effects include solute segregation prior to precipitation and haphazard shifting of certain matrix planes required to form the precipitate.* Solute segregation may cause local variations in either lattice parameter or atomic scattering power. Errors in periodicity and also particle size limitations may produce indefinite periodicities in the precipitate structure. If this powerful technique is to be useful for studies of the mechanism of precipitation, of nucleation and of crystal growth, and is to contribute to the theory of age-hardening, all possible causes must first be understood before the correct choice of a general interpretation can be made.

In interpreting the diffraction effects, the authors favor the concept that the controlling factor is particle size alone. Before considering the evidence in favor of this interpretation, the limitations of other explanations that have been advanced should be considered from the general standpoint, founded on the data for all systems of alloys that have been investigated. For example, enrichment of certain plate-like areas in solute atoms parallel to the Widmanstätten planes of the matrix *without* any change of lattice type was advanced for explaining the diffraction effects of Al–Cu alloys (Calvet *et al.* 1939; Preston, 1938*a*, *b*, 1940). If the difference in scattering power of the atoms alone is considered responsible, then this explanation cannot be general, for it cannot explain similar diffraction effects observed for Al–Mg alloys (Geisler *et al.* 1943*b*); since the scattering powers of Al and Mg atoms are little different, a cluster enriched in Mg atoms would diffract little differently from the general matrix, and the observed prominent streaks would not be expected. A somewhat similar interpretation is based upon local changes in lattice parameter provided by agglomeration of solute atoms. According to this concept, regions of high solute concentration, with lattice parameters slightly different from those of the matrix but with the same lattice type, are responsible for these diffraction effects. In view of the prominent streaks observed for Al–Ag, this alone cannot be a general interpretation, since concentration gradients in this alloy could not provide detectable variations in lattice parameters. The aluminum and silver atoms are so similar in radii that a change in the lattice parameter of aluminum has not been detected on adding as much as 40–50 % silver in solid solution. Unfortunately, a precipitation alloy has not yet been studied in which both atomic scattering power and radii of solvent and solute are nearly the same; nevertheless, the diffraction effects cannot be generally associated with the matrix structure.

The most conclusive evidence in favor of the interpretation based on precipitate structure is presented in this paper. This is the evolution of reciprocal-lattice points for the precipitate from the configurations for the earlier stages in the aging of the Al–Mg–Si alloy. The platelet rods are not associated directly with matrix points but resolve on further aging into points for the transition lattice. Therefore, the platelets can be regarded as particles of the precipitate with a different lattice type from that of the matrix. A new structure has been formed within the matrix crystal.* On the basis of this interpretation the rods should be considered relative to the reciprocal points for thick precipitate particles and not relative to the matrix points.

In the less complicated Al–Cu and Al–Ag alloy systems that have been investigated previously, the reciprocal-lattice rods usually pass through points for matrix planes. Thus, the assumption of lack of periodicity in the matrix seemed justified. But consider the alternative. Evidence in favor of the precipitate as the source of the indefinite periodicity has been presented earlier for Al–Ag. When the rods are regarded relative to the points for thick precipitate particles, as in Fig. 11, the rods pass through precipitate points also, and these may be considered to evolve from the rods as observed for Al–Mg–Si. The presence of subsequent points for the precipitate in the Al–Ag alloy near matrix points, and the alignment of these because of coherency, account for the rods passing through matrix points. On this basis, uncertainty of periodicity is not in the four ⟨111⟩ directions of the matrix planes but in the ⟨00.1⟩ direction of the four differently oriented precipitate particles. Because of the Widmanstätten relations, these directions coincide. Such considerations when applied to the early structures of Al–Cu alloys will probably explain the presence of reciprocal-lattice rods extending on only one side of the matrix points (Preston, 1938*a*, *b*, 1940). Here again, coherency of the transition structure with the matrix results in the points for the precipitate being in line with and adjacent to those of the matrix. In the platelet stage the rods are centered at potential precipitate points, near to but not at matrix points. As the particles grow, the rods develop into precipitate points. Although the structure of Al–Mg alloys has not been fully analyzed, it too, like Al–Mg–Si, contains

* Diffraction effects associated with the transformation in cobalt have been interpreted this way. It has also been suggested for other reactions in which a hexagonal structure is formed from a face-centered cubic structure (Barrett & Geisler, 1940). Perhaps particle-size limitations of the new phase will adequately explain the diffraction phenomena with cobalt also.

* A distinction may not be clear when both phases have the same lattice type (i.e. Cu–Ag, Ni–Au) and strained transition structures are formed.

platelets of a structure distinctly different from the matrix, since many of the rods are not near matrix points. All these data are consistent with the indefinite periodicity being in a certain crystallographic direction of the precipitate platelet structure and not necessarily of the matrix structure.

Whether the reciprocal-lattice rods are due to lack or imperfection of periodicity in the precipitate structure, or merely to a limited dimension, can be decided from the physical shape of the particles without involving any appreciable extrapolation along the size scale. For example, microscopic examination has shown that when the particles are resolvable they generally are plate-like *with their smallest dimension in the direction of the uncertain periodicity* of the earlier stages. At this stage they produce normal three-dimensional Bragg diffraction. At the much earlier stage, when they produce rods in the reciprocal lattice, the particles are resolvable only with the electron microscope (Geisler & Keller, 1947), and they also are observed to be plate-like. When first detectable with the electron microscope their true shape is probably not discernible, but their maximum dimension appears to be about 100 A. Even this dimension is well within the range at which particle size affects line broadening so that the thickness dimension, which is about one-tenth of the lateral dimension (when microscopically resolvable), is much less than that required for good resolution of X-rays. The Laue condition is relaxed in this direction because of limited thickness; the plane spacings through the thickness are not determinable. An imperfection or lack of periodicity in this direction may exist, but it would not be discernible because of the small thickness, and is not detected when the precipitate particles have grown thick. Judging from the relatively large span (thousands of atom distances) between precipitate particles when they are microscopically resolvable, it is difficult to conceive sufficiently intense super-lattice-like diffraction effects from the matrix due to a regular insertion of the thin platelets in the sequence of matrix planes. Thus combined X-ray diffraction and microscopic examinations reveal that the reciprocal-lattice rods could be due generally to precipitate particles of limited thickness. These platelets have an indeterminate periodicity normal to their plane which is best regarded as unresolvable owing to the small thickness rather than to lack or imperfection of periodicity.

### 8. Contribution to the theory of precipitation

The adoption of a general interpretation of diffuse diffraction effects for aged alloys can now be justified. While interpretations based on matrix structure have been adequate for some alloys, the diffraction effects in other alloys are best explained only in terms of precipitate structure and limited crystal dimensions. Thus a general interpretation based on matrix structure is not possible. Certainly, the atomic movements required to form the new phase are not the same in all precipitating systems; however, there is the one general feature: *the particles in all systems grow from submicroscopic sizes.* Usually the particles are not equiaxed, and frequently they are plate-like. On this basis, dimension limitations are to be expected during the course of growth, as pointed out in the introduction to the paper. Such an interpretation adequately explains the presence of rods in reciprocal lattices of all alloy systems that have been investigated. It is a simple interpretation equally applicable to configurations which occur at stages prior to the rods.

The stringlet stage is a new concept which is first reported here for the two alloys Al–Ag and Al–Mg–Si. If one wishes to indicate the aging sequence by stages such as: matrix → 'Guinier-Preston zone or aggregate' (platelet) → coherent transition structure → equilibrium structure (Mehl & Jetter, 1940), then the stringlets precede the Guinier-Preston zone. The nature of the stringlet stage can be determined from its reciprocal-lattice representation relative to that of the platelet stage. Since the platelet rods evolve from the stringlet plane areas in the reciprocal lattice, then the stringlets can be considered as platelets with an indefinite periodicity or relaxed Laue condition in one of their two prominent dimensions. This corresponds to a relaxation of two Laue conditions for thick precipitate particles. The stringlets then are simply precipitate particles in which only one dimension is sufficiently large to afford sharp X-ray diffraction.

That one direction in the Widmanstätten plane in Al–Ag alloys should dominate any other direction of growth is a rather unexpected observation. Plate-like growth of particles is explained by preferred growth in the plane which involves least strain (best matching of atom sites of matrix and second-phase structures) and retarded growth normal to this plane where matching is poor. In Al–Ag alloys the matching in the (00.1) $\gamma$ plane with the (111) matrix plane is equally good in all lateral directions. Thus no direction in this plane is favored by least strain, and on the basis of this criterion preferred growth in one direction would not be expected. But particles which have one prominent dimension are detected in the early stages of growth. In the Al–Ag crystal they are along ⟨110⟩ directions, and in the Al–Mg–Si alloy they are along ⟨100⟩ directions of the matrix crystal. These directions are common to the planes of two or more platelet orientations (Fig. 24), and probably for this reason they are chosen for initial growth. Perhaps the theory of nucleation will have to account for the early shape, with later shape only predictable from disregistry considerations. A pair of atoms in line may make it easier for the next one to join that line rather than to go along a second line in the plane. (This is the same sort of reasoning that has been applied sometimes to planar growth versus equiaxed growth.) Preferential growth of the precipitate in one direction would persist

on this basis as long as the particles were small, but as they become larger and more and more solute atoms become attached to the edge of the particle such a tendency would diminish, and uniform lateral growth (promoted by planar coherency) would be attained.

Growth in the thickness direction in which the strains are greatest is much slower compared with that in both lateral dimensions. At the well-defined stringlet stage the particles in the Al–Mg–Si alloy are probably 10 by 20 by $>100$ A., while at the platelet stage they are 15 by $>100$ by $>100$ A. After the lateral dimensions exceed the limit of resolution, differences in these dimensions are not detectable, so that any reflection of the initial preferential growth on lateral shape cannot be ascertained at the platelet stage; however, when

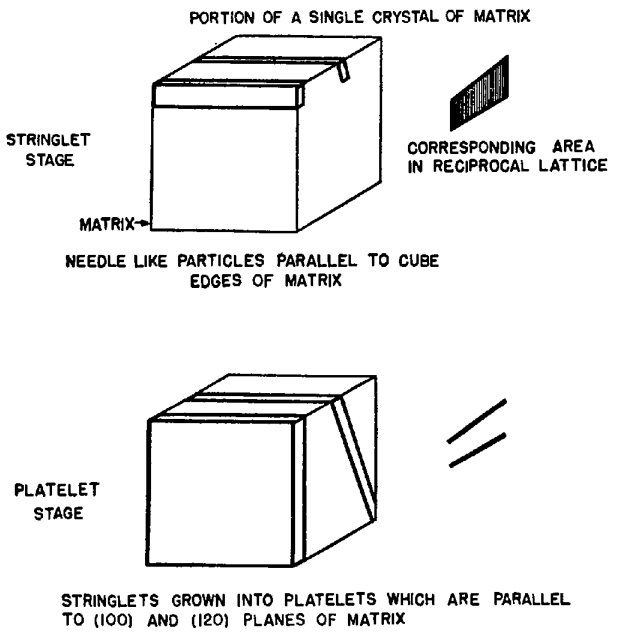


Fig. 24. An interpretation of structure of aged Al–Mg–Si alloy.

the particles in Al–Mg–Si are resolvable with the microscope some are square but others are rectangular tablets. In some alloy systems preferred unidirectional growth persists, and the particles are truly needle-like when they have grown large enough to resolve with the light microscope.

The earliest stage of precipitation that could possibly be detected by X-ray diffraction is suggested at the bottom of Fig. 18. This is the stage at which the particles are below the limit of resolution in all three directions. Indeed, patterns have been observed which could be interpreted as indicating this stage. Diffuse halos have been observed about matrix reflections in patterns for an Al–Ag alloy made with monochromatic X-rays (Guinier, personal communication). Consider the surroundings of matrix points in the reciprocal lattice for Al–Ag—for example, the $002M$ point in Fig. 11. When each of the precipitate points here is replaced by a diffuse volume, these would blend in such a manner that this matrix point is surrounded by a hollow diffuse volume. This could explain the observed diffraction. Intense diffraction about the direct beam, as in Fig. 14 A–C, is also evidence for this earliest stage, but here at (000) the volumes for all the orientations of precipitate are superimposed, and that for a single orientation cannot be isolated for a study of particle shape. Thus, with the proposed general interpretation based on dimension limitations and the described method of analysis, the precipitation process can be traced back to its beginning from a few unit cells.

In conclusion, a few words concerning terminology should be added. While the terms 'platelet' and 'stringlet' are convenient for describing the sources of the X-ray diffraction effects, they are not used to imply discrete steps in the precipitation process but should be regarded only as a consequence of the limitations of the X-ray diffraction technique. The impression that the particles first grow as needles and then suddenly become plates is not intended. They grow anisotropically, and as each dimension reaches the limit of resolution a Laue condition is added until the last dimension is resolved when the particles diffract as normal three-dimensional gratings according to Bragg's law. Thus these so-called 'stages' are all considered to represent the gradual and continuous growth of the precipitate according to the reaction: matrix → coherent transition lattice. On the other hand, the change from the transition lattice to the equilibrium structure is a discrete step and may occur at any degree of growth of the precipitate. The transition lattice is most conveniently detected when the transformation does not occur until after the precipitate has grown to a resolvable thickness, for then the lattice constants can be determined by the usual X-ray diffraction methods. To supplement these, the analysis described here can be used to provide some information about the transition structure if coherency is lost early in the precipitation process. The geometry of the rods or plane areas in the reciprocal lattice relative to matrix points and subsequent points for the second phase provides such information.

The authors wish to express their gratitude to Dr C. S. Barrett, of the Institute for the Study of Metals, University of Chicago, for profitable discussions during the course of this research and for helpful comments on the manuscript. The valuable comments of Dr R. F. Mehl and Dr R. Smoluchowski, of the Carnegie Institute of Technology, and also Dr D. Harker, of the General Electric Research Laboratory, are greatly appreciated.

## References

BARRETT, C. S. (1943). *Structure of Metals*. New York: McGraw Hill.

BARRETT, C. S. & GEISLER, A. H. (1940). *J. Appl. Phys.* **11**, 733.

BARRETT, C. S., GEISLER, A. H. & MEHL, R. F. (1941). *Trans. Amer. Inst. Min. (Metall.) Engrs*, **143**, 134.
CALVET, J., JACQUET, P. & GUINIER, A. (1939). *J. Inst. Met.* **65**, 121.
EWALD, P. P. (1940). *Proc. Phys. Soc. Lond.* **52**, 167.
GEISLER, A. H., BARRETT, C. S. & MEHL, R. F. (1943*a*). *Trans. Amer. Inst. Min. (Metall.) Engrs*, **152**, 182.
GEISLER, A. H., BARRETT, C. S. & MEHL, R. F. (1943*b*). *Trans. Amer. Inst. Min. (Metall.) Engrs*, **152**, 201.
GEISLER, A. H. & KELLER, F. (1947). *Trans. Amer. Inst. Min. (Metall.) Engrs*, **171**, 192.
GUINIER, A. (1942). *C.R. Acad. Sci., Paris*, **214**, 34.
GUINIER, A. (1943). *Métaux, Corrosion-Usure*, **18**, 209.
GUINIER, A. (1946). *Mesures*, **11**, 305.
GUINIER, A. & JACQUET, P. (1943). *C.R. Acad. Sci., Paris*, **217**, 22.
GUINIER, A. & JACQUET, P. (1944). *Rev. Métall.* **41**, 1.
GUY, A. G., BARRETT, C. S. & MEHL, R. F. (1948). *Metals Tech.* **15**, 2.
MEHL, R. F., BARRETT, C. S. & RHINES, F. N. (1932). *Trans. Amer. Inst. Min. (Metall.) Engrs*, **99**, 203.
MEHL, R. F. & JETTER, L. K. (1940). *Symposium on Age-Hardening of Metals*, p. 342. Cleveland: American Society for Metals.
PRESTON, G. D. (1938*a*). *Phil. Mag.* **26**, 885.
PRESTON, G. D. (1938*b*). *Proc. Roy. Soc.* A, **167**, 526.
PRESTON, G. D. (1940). *Proc. Phys. Soc. Lond.* **52**, 77.

*Acta Cryst.* (1948). **1**, 252

# The Crystal Structure of *p*-Nitroaniline, $NO_2.C_6H_4.NH_2$

BY S. C. ABRAHAMS AND J. MONTEATH ROBERTSON
*The University, Glasgow W. 2, Scotland*

(*Received* 28 *June* 1948)

*p*-Nitroaniline forms monoclinic crystals, space group $C_{2h}^5$–$P2_1/n$, with four asymmetric molecules in the unit cell. A quantitative X-ray investigation based on visual intensity measurements of about 250 reflexions from the axial zones has led to a complete determination of the structure, and the results have been refined by the double Fourier series method, which gives projections of the structure along the three crystal axes. The co-ordinates of the atoms, the molecular dimensions, and the intermolecular distances are given. The nitro-group is symmetrical and lies in the plane of the benzene ring. In addition to rather weak hydrogen bridges connecting the oxygen atoms of the nitro-group to the amino-groups of adjoining molecules, there is a very close approach (2·7–3·0 A.) between one of the nitro-oxygen atoms and three of the aromatic carbon atoms of an adjoining molecule. This appears to be an intermolecular attraction of a new type, and it is suggested that a similar mechanism may be responsible for the formation of a large class of the molecular compounds that are formed between aromatic nitro-compounds and polycyclic hydrocarbons.

## Introduction

The structure of the nitro-group in aromatic compounds has been the subject of a number of recent studies, but the results show considerable variation. Thus, the N–O distances have been reported as 1·41 and 1·21 A. in 4:4′-dinitrodiphenyl (van Niekerk, 1942), equal at 1·19 A. and also at 1·20 A. in *m*-dinitrobenzene (Gregory & Lassettre, 1947; Archer, 1946), 1·25 and 1·10 A. in *p*-dinitrobenzene (James, King & Horrocks, 1935), and equal at 1·23 A. in the same compound (Llewellyn, 1947). The values assigned to the O–N–O valency angle vary from 116 to 130° in the same studies, and the C–N distances from 1·41 to 1·54 A. Further work on simple nitro-compounds is therefore required, and the present study is a contribution to this field.

The crystal structure of *p*-nitroaniline is also of special importance in the study of intermolecular attractions and the formation of molecular compounds. It will be shown that the compound displays certain abnormal properties, and that these appear to be explained by a new type of rather powerful attraction between an oxygen atom of the nitro-group and the aromatic carbon atoms of an adjacent molecule in the crystal structure. Judged by the approach distances (2·6–3·0 A.) these attractions are equivalent to the stronger types of hydrogen bridge and probably afford an explanation of the formation of certain large classes of aromatic molecular compounds.

## Analysis of the structure

*Crystal data.* *p*-Nitroaniline, $NO_2.C_6H_4.NH_2$; $M$, 138·1; m.p. 147·5° C.; $d$, calc. 1·422, found 1·418; monoclinic prismatic; $a=12{\cdot}34\pm0{\cdot}02$, $b=6{\cdot}02\pm0{\cdot}02$, $c=8{\cdot}63\pm0{\cdot}02$ A., $\beta=91°\,40'$. Absent spectra, $(h0l)$ when $h+l$ is odd; $(0k0)$ when $k$ is odd. Space group, $C_{2h}^5$–$P2_1/n$. Four molecules per unit cell. No molecular symmetry required. Volume of the unit cell, 640·7 A.$^3$